Locating the boundary between the Pleistocene and the Holocene in Chinese loess using luminescence

Zhong-Ping Lai[1]* and Ann G. Wintle[2]

([1]Centre for the Environment, University of Oxford, South Parks Road, Oxford OX1 3QY, UK; [2]Institute of Geography and Earth Sciences, University of Wales, Aberystwyth SY23 3DB, UK)

Received 27 October 2005; revised manuscript accepted 16 February 2006

A HOLOCENE RESEARCH REPORT

Abstract: A detailed chronology has been obtained for a loess section at Yuanbao, situated at the northwestern edge of the Chinese Loess Plateau. The ages were obtained by the measurement of the optically stimulated luminescence (OSL) from coarse-silt-sized quartz grains. These ages showed that deposition at this site was continuous from 17 ka to the present, but that there was a decrease in the sedimentation rate from 0.60 to 0.10 m/ka at 13.48 ± 1.15 ka, and this is proposed as the location of the Pleistocene/Holocene (P/H) boundary. A change in OSL sensitivity occurs at this depth. The depth and sharpness of this boundary is compared with the change obtained in low-field magnetic susceptibility (MS) measurements on 65 samples from the section. The MS changes gradually over 1.9 m and thus does not provide an easily discernible boundary. The new OSL-based sedimentation rates are used to calculate the mass accumulation rates for the Holocene and the end of the Pleistocene.

Key words: Chinese loess, Pleistocene/Holocene boundary, sedimentation rate, luminescence chronology, quartz OSL, optically stimulated luminescence, magnetic susceptibility.

Introduction

Loess in the Chinese Loess Plateau (CLP) provides continuous records of palaeoenvironmental change during the whole Quaternary period (Liu, 1985; Kukla, 1987; Kukla *et al.*, 1988; Kukla and An, 1989; Ding *et al.*, 1994; Lu *et al.*, 1999; An, 2000). One such record is provided by the low-field magnetic susceptibility (MS), which is stronger in the palaeosols than in the loess (Maher and Taylor, 1988; Zhou *et al.*, 1990; Maher *et al.*, 1994). MS values in the loess–palaeosol sequences fluctuate in parallel with the oxygen-isotope ($\delta^{18}O$) oscillations derived from marine sediments (Kukla, 1987; Kukla *et al.*, 1988; An *et al.*, 1991), for which the chronology has been developed by a combination of numerical dating and astronomical tuning (Imbrie *et al.*, 1984; Martinson *et al.*, 1987). Thus, the chronological framework for loess–palaeosol sequences is mainly dependent on matching the MS peaks with peaks in the marine $\delta^{18}O$ records, with a few age controls being provided by magnetic reversal boundaries (Liu, 1985; Kukla, 1987). Such correlations require that hiatuses do not occur in the terrestrial record. It is also assumed that palaeosols represent syn-depositional pedogenic processes that are the result of climatic factors (Pye, 1995). However, the transition between high and low MS values is not sharp. This implies that the stratigraphic boundary as defined by the MS signal will be time-transgressive, depending upon the rates of weathering and dust deposition at each site. Sediment supply is also likely to be important in controlling palaeosol formation and this may vary out of phase with climate change (Kemp, 2001). If the sediment accumulation rate is low during a period of pedogenesis, then this may result in postdepositional changes in the underlying loess. Such effects of pedogenesis on the loess underlying the last interglacial palaeosol (S_1) at Yuanbao in the Linxia basin (YB in Figure 1) were reported by Feng *et al.* (2004a) in a study of the MS record. In a similar study at Shagou section (37°33′N, 102°49′E, 135 km to the northeast of Xining), Wu *et al.* (2002) found the effect of pedogenesis to extend about 40 cm into the loess (L_2) underlying the last interglacial palaeosol. However, it is difficult to differentiate between pedogenic penetration into the loess and the effect of weak climatic warming, prior to the arrival of a full interglacial climate.

It is possible to obtain separate information on the sedimentary process (ie, the deposition of the mineral grains) and the effects of pedogenic processes. These different processes can be investigated most effectively by looking at the

*Author for correspondence at: Faculty of Geography, University of Marburg, D-35032 Marburg, Germany (e-mail: zhongping.lai@staff.uni-marburg.de, or zplai@yahoo.com.cn)

10.1191/0959683606hol980rr

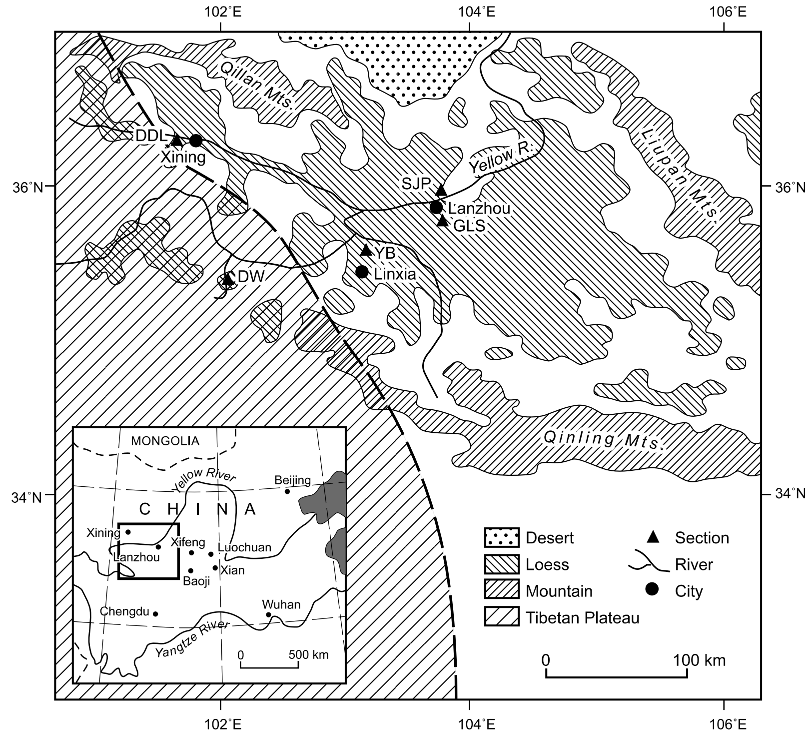

Figure 1 Map showing the Chinese Loess Plateau and the location of Yuanbao (YB) section, and other sections referred to in the text (modified from Chen *et al*., 1997 and reprinted with permission from Elsevier). DDL, Dadongling; DW, Duowa; GLS, Gaolanshan; SJP, Shanjiaping

relevant properties of the sediment that spans the Pleistocene/Holocene (P/H) boundary. In previous studies, grain-size has been used as a proxy for changes in depositional processes caused by the relative dominance of the winter monsoon regime (eg, Porter and An, 1995; Xiao *et al*., 1995). In particular, changes in grain size have been interpreted in terms of changes of wind strength (Liu, 1985). In contrast, low-frequency magnetic susceptibility has been used as a proxy for pedogenic processes related to the dominance of the summer monsoon regime (eg, An *et al*., 1991). However, at most sections the boundary is not well defined. Pedogenesis also causes colour changes, with the 'greyscale' intensity being used to provide a quantitative record of climate change (Porter, 2000; Chen *et al*., 2002). However, the colour change defined by greyscale intensity between a palaeosol and the underlying loess is gradual, taking several tens of centimetres for the transition from loess to palaeosol and once again the boundary is hard to determine.

In this paper, optically stimulated luminescence (OSL) dating of the coarse-silt-sized grains is used to determine the depth of the change in sedimentation rate between the end of the Pleistocene and the Holocene for a loess section at Yuanbao on the northwestern edge of the CLP. This depth is compared with the magnetic susceptibility (MS) record measured for samples from the dated section, and previously published grain-size data for part of the Yuanbao section. In addition, these sedimentation rates can be converted into mass accumulation rates. The values obtained can be compared with those obtained in a previous compilation of data for the CLP (Sun *et al*., 2000). From this compilation it was concluded that dust deposition during the most recent interglacial, the Holocene, equivalent to Marine Isotope Stage (MIS) 1, is five times less than at the end of the Pleistocene, equivalent to MIS 2. However, the main aim of this study is to locate the P/H boundary as defined by a change in sedimentation rate given by OSL dating and to compare its position with that suggested by MS observations.

Yuanbao section

For this study, a site was chosen at the northwestern edge of the CLP, where the sedimentation rate would be expected to be several times higher than in the central part of the CLP (eg, at Luochuan). The Yuanbao section (site CH02/2) (35°38′23.3″N, 103°08′50.2″E, elevation 2177 m) is located in the Linxia basin, about 120 km southwest of Lanzhou city, near the city of Linxia (YB in Figure 1). It lies close to the eastern edge of the Qinghai-Xizhang (Tibetan) Plateau, and adjacent to the Tengger Desert to the north. Up to 42 m of loess was deposited in the last 130 ka (Chen *et al*., 1997, 1999), resulting in an average sedimentation rate of about 0.3 m/ka; such a high rate permits high-resolution palaeoclimatic data to be obtained. Chen *et al*. (1997) presented MS (at 5 cm intervals) and grain size (at 10 cm intervals) measurements for the uppermost 35 m of sediment; in a subsequent study they presented data for loessic sediment occurring at a depth of 30 to 42 m, where the last interglacial palaeosol (equivalent to MIS 5) was recorded in detail (Chen *et al*., 1999).

In the present study, we have investigated only the uppermost 4.5 m of the section (CH02/2) at Yuanbao. This spans the whole of the Holocene and the most recent part of the Pleistocene; the pre-existing chronology was based on two radiocarbon dates on organic matter (6070 $\pm$ 80 yr BP at 1.05 m and 13 360 $\pm$ 340 yr BP at 3.70 m) (Chen *et al*., 1996). These ages were quoted in the compilation of numerical ages (Sun *et al*., 2000) used to obtain mass accumulation rates across the CLP (Kohfeld and Harrison, 2003). Based on our (ZPL) observation of the colour change in the field, the boundary between the Holocene soil S_0 and the Pleistocene loess L_1 is at 2.4 m below the surface. In this study 12 luminescence samples and 88 magnetic susceptibility samples were collected from a single section (site CH02/2), which is a 4.5 m high exposure beside a road.

Magnetic susceptibility data

Low-field magnetic susceptibility (MS) measurements were made in the laboratory, using samples taken at 5 cm intervals from 0 to 2.7 m and at 20 cm intervals from 2.7 to 4.5 m (Figure 2b). The measurement procedure was the same as that used for the loess and palaeosols of the last 130 ka at Luochuan (location was shown in inset in Figure 1) (An *et al*., 1991). At Yuanbao, the MS values increased from 2.4 m to 0.5 m (Figure 2b) with the change thus taking place over 190 cm. Similar gradual changes in MS signal have been reported by others elsewhere across the CLP for the S_0/L_1 transition, eg, over about 200 cm at Luochuan (Heller *et al*., 1993; An and Porter, 1997), over about 150 cm in well A at Gaolanshan (GLS in Figure 1), near Lanzhou (Derbyshire *et al*., 1995), and over about 200 cm at Shajiaping (SJP in Figure 1), near Lanzhou (Fang *et al*., 1999).

Since the change takes place over 1.9 m, it is impossible to locate the H/P boundary at Yuanbao with any precision using MS (Figure 2b). If the centre point of the change in MS is used, the boundary would be at about 1.45 m; if the point of most rapid change in MS is taken as the boundary, then it is at about 1.30 m; if the onset of change is taken, then it is at about 2.4 m, coincident with the field-observed colour change. None of these positions can be defined with any rigour. For this paper, the MS-defined P/H boundary is taken to be at 1.30 m (Figure 2b).

Optically stimulated luminescence dating

Optical dating of the mineral grains that make up the bulk of the loess allows absolute ages to be determined and sedimentation rates to be calculated. The natural OSL signal of the quartz grains provides a measure of the time when the grains were deposited. The development of the Single Aliquot Regeneration-dose (SAR) protocol (Murray and Wintle, 2000) for OSL dating of quartz has made it possible to establish high-resolution chronologies in loess deposits. Roberts *et al*. (2001) have demonstrated that a change in sedimentation rate can be observed using high-resolution OSL dating of Holocene dust deposits from Duowa (DW in Figure 1) to the west of Yuanbao, though in their case the cause of the change was anthropogenic activity.

Sample preparation and equipment for OSL measurement

The luminescence samples were collected in *c*. 5 cm × 5 cm × 5 cm blocks at intervals of 33 cm. In subdued red light in the laboratory, the daylight-exposed outer layer was removed for dose-rate measurements. The remaining core was treated with HCl and H_2O_2, and the 45–63 μm fraction separated by sieving. This fraction was treated with 35% hydrofluorosilicic acid (Berger *et al*., 1980) for about two weeks to dissolve feldspars and then with 10% HCl for about 30 min to remove any acid-soluble fluoride precipitates. This treatment is thought not to affect the quartz grains, thus leaving an alpha-irradiated layer (~ 10 μm thick) on the surface of each grain. About 4 mg of quartz grains were then fixed using silicone oil onto an area of 0.8 cm diameter on 1.0 cm diameter stainless steel discs. The purity of the isolated quartz was tested on a few aliquots by IR (830 nm) stimulation; no IRSL was observed.

Experiments were carried out using a Risø TL-DA-15 reader, incorporating blue diodes ($\lambda = 470 \pm 20$ nm) and an infrared (IR) laser diode ($\lambda = 830 \pm 10$ nm) (Bøtter-Jensen *et al*., 2000). The OSL measurements were made using 470 nm stimulation at 130°C for 50 s, and OSL was detected using two 3 mm thick U-340 filters (detection window 275–390 nm) in front of the photomultiplier tube. Irradiations were carried out using a $^{90}Sr/^{90}Y$ beta source within the Risø reader; the dose rate of the source (6.233 ± 0.181 Gy/min) was obtained using OSL measurements on quartz of the same grain size that had been gamma irradiated at the National Physical Laboratory (UK).

Laboratory dose recovery test

The suitability of a procedure for equivalent dose (D_e) determination was checked with a 'dose recovery test' (Murray and Wintle, 2003); in this test, the procedure is applied to an aliquot that has been given a laboratory dose following appropriate resetting of the luminescence. This test examines the combined function of all the conditions of the procedure, such as the preheats, size of test dose, etc. A dose recovery test

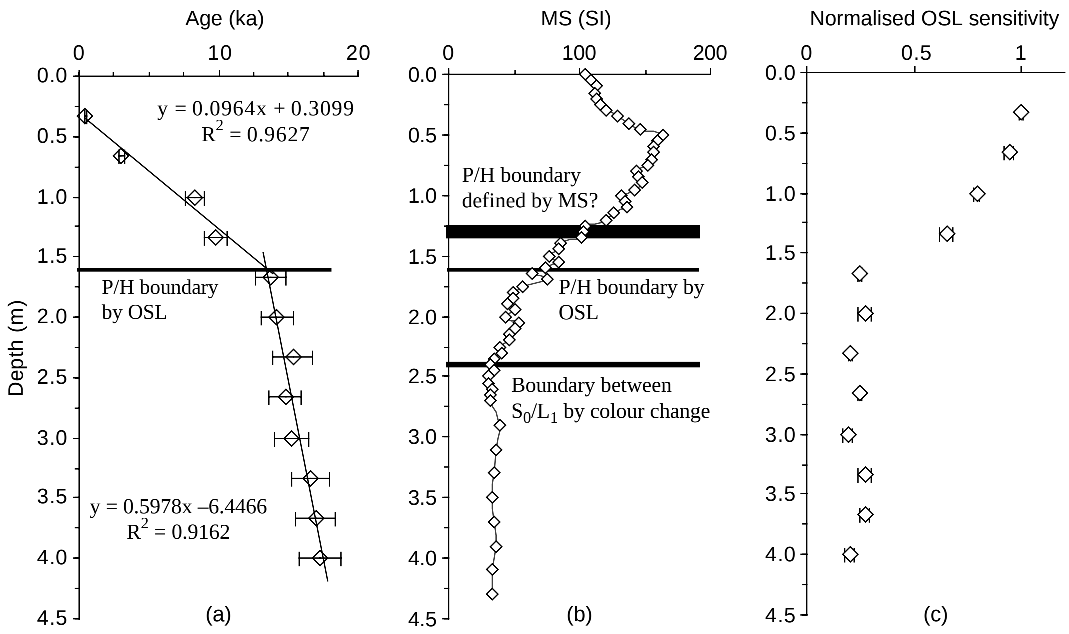

Figure 2 Experimental results for YB section. (a) Dating results, (b) MS curve and (c) relative quartz OSL sensitivity

was performed on two representative samples, CH02/2/3 and CH02/2/10. The OSL signal of all aliquots was reset by bright sunlight for 10 min, before the aliquot received a laboratory dose. The preheat used was 260°C for 10 s. Test doses of 4.8 Gy and 28.5 Gy were used for samples CH02/2/3 and CH02/2/10, respectively; the preheat following delivery of the test dose was 220°C for 10 s, stronger than 160°C for 0 s previously used in dating loess (Roberts and Wintle, 2001; Watanuki *et al*., 2003). This is to ensure that if any laboratory-dose-induced ultra-fast OSL component exists, it is removed by the thermal treatment to avoid potential D_e underestimation (Jain *et al*., 2003). For CH02/2/3, the given laboratory dose was 19.2 Gy, and the measured value obtained for 12 aliquots was 18.6 ± 0.3 Gy. For CH02/2/10, the given laboratory dose was 52 Gy, and the measured value for 12 aliquots was 50.2 ± 0.7 Gy. Thus, the ratios of the given to the measured dose were 1.03 ± 0.02 and 1.04 ± 0.01, respectively.

Equivalent dose determination

Since the known laboratory dose was recovered within 5%, the same experimental conditions were adopted for dating all the samples. Equivalent dose (D_e) was determined using doses chosen to bracket the value of D_e expected from results of a test run. A zero dose was used to detect recuperation, and a repeated dose was given for the recycling test (Murray and Wintle, 2000). The test dose was 4.8 Gy for the four younger samples in the upper part of the section, but it was changed to 28.5 Gy for the older eight samples in the lower part of the section because of their lower OSL sensitivity. The OSL signal of the first 0.4 s stimulation (background subtracted) was integrated for D_e calculation. The error in a single D_e value for an aliquot was estimated using Monte Carlo simulation; the final D_e for a sample was the unweighted mean of D_es for many aliquots and the standard error of the mean D_e was estimated from the D_e distribution of a set of aliquots. For all 12 samples, the average recuperation value was 0.020 ± 0.004%, which is negligible, and the average recycling ratio was 1.02 ± 0.02, identical within errors to the ideal value of 1.

The D_e values, and the number of aliquots used, are given in Table 1. This table also gives the concentrations of uranium, thorium and potassium as measured by Inductively Coupled Plasma Mass Spectrometry (ICP-MS) (Bailey *et al*., 2003). The alpha efficiency value was taken as 0.040 ± 0.002, as obtained for fine-grained quartz by Rees-Jones (1995). The water content (water/wet sediment) was taken as 10 ± 5% for loess samples and 15 ± 5% for palaeosol samples. The cosmic-ray dose rate was estimated for each sample as a function of depth, altitude and geomagnetic latitude (Prescott and Hutton, 1994). The OSL ages are listed in Table 1 and presented in Figure 2a. The ages are consistent with the calibrated radiocarbon age ranges of 6.79 to 7.02 ka at about 1.05 m and 15.18 to 16.08 ka at about 3.70 m (values taken from Sun *et al*., 2000).

Quartz OSL sensitivity

The OSL sensitivity of the 45–63 μm grains can be expressed as the total signal output (integrated from 0 to 50 s, and with the average background subtracted) per unit dose and per unit mass. During the dating analysis, it was found that the OSL sensitivity of the four samples from the upper part of the section was higher than that of the lower samples; this had led to the use of higher test doses for the lower eight samples (28.5 Gy, rather than 4.8 Gy). From the dating results, it can be deduced that the OSL sensitivity of samples of Holocene age is higher than that for those dating from the end of the Pleistocene. The values can be compared provided that the aliquots are weighed with adequate precision and that there is no difference between aliquots in terms of the different OSL components (Jain *et al*., 2003). Additional systematic measurements have been performed to quantify the OSL sensitivity for each of the 12 samples. Four aliquots (of about 4–5 mg and weighed to ± 0.01 mg) were made for each sample. Each aliquot was then: (1) bleached by blue (470 nm) light for 100 s at 130°C; (2) given a fixed dose of 20 Gy; (3) heated to 220°C (and held at 220°C for 10 s); (4) exposed to IR stimulation at room temperature for 20 s; (5) stimulated using blue (470 nm) light for 50 s at 130°C to obtain the OSL signal. Step 4 is to check for any feldspar contamination; for no aliquot was significant IRSL found. The OSL sensitivities were normalized to that of sample CH02/2/1 and the results are shown in Figure 2c. The sensitivity decreases gradually from 0.33 to 1.33 m depth, drops more sharply between 1.33 m and 1.66 m, and then remains relatively constant from 1.66 to 4.0 m. Thus it appears that, in the absence of numeric age control, the OSL sensitivity can be used to allocate a sample to either the Holocene or the Pleistocene. However, it should be noted that the change is not a step function (Figure 2c).

Determination of Pleistocene/ Holocene boundary at Yuanbao using OSL dating

The OSL ages obtained for samples taken from the section suggest that the sedimentation rate changed dramatically at a

Table 1 Environmental radioactivity and dating results

Sample ID	Depth (m)	K (%)	U (ppm)	Th (ppm)	Water content (%)	D_e (Gy)	Aliquot number	Dose rate (Gy/ka)	Age (ka)
CH02/2/1	0.33	1.89 ± 0.07	2.53 ± 0.04	12.39 ± 0.26	15 ± 5	1.47 ± 0.20	12	3.31 ± 0.25	0.44 ± 0.06
CH02/2/2	0.66	2.02 ± 0.08	2.43 ± 0.05	11.95 ± 0.22	15 ± 5	10.2 ± 0.2	12	3.34 ± 0.25	3.1 ± 0.2
CH02/2/3	1.00	1.71 ± 0.12	2.46 ± 0.04	12.18 ± 0.19	15 ± 5	25.7 ± 0.3	12	3.10 ± 0.25	8.3 ± 0.6
CH02/2/4	1.33	1.88 ± 0.12	2.57 ± 0.06	11.71 ± 0.26	15 ± 5	31.6 ± 0.7	12	3.22 ± 0.26	9.8 ± 0.7
CH02/2/5	1.66	1.74 ± 0.10	2.39 ± 0.05	11.80 ± 0.15	15 ± 5	44.2 ± 1.2	10	3.22 ± 0.23	13.7 ± 1.0
CH02/2/6	2.00	1.90 ± 0.06	2.39 ± 0.06	11.94 ± 0.26	15 ± 5	46.3 ± 1.4	10	3.26 ± 0.23	14.2 ± 1.0
CH02/2/7	2.33	1.80 ± 0.11	2.52 ± 0.05	11.39 ± 0.15	10 ± 5	50.6 ± 2.3	11	3.30 ± 0.26	15.3 ± 1.3
CH02/2/8	2.66	1.86 ± 0.09	2.41 ± 0.07	10.68 ± 0.20	10 ± 5	48.2 ± 1.2	12	3.26 ± 0.25	14.8 ± 1.1
CH02/2/9	3.00	1.81 ± 0.05	2.43 ± 0.08	10.79 ± 0.29	10 ± 5	49.1 ± 1.3	12	3.22 ± 0.25	15.2 ± 1.1
CH02/2/10	3.33	1.72 ± 0.12	2.47 ± 0.04	10.78 ± 0.23	10 ± 5	52.2 ± 1.5	12	3.14 ± 0.25	16.6 ± 1.3
CH02/2/11	3.66	1.89 ± 0.09	2.52 ± 0.09	10.29 ± 0.13	10 ± 5	55.3 ± 1.8	12	3.26 ± 0.25	16.9 ± 1.3
CH02/2/12	4.00	1.91 ± 0.13	2.49 ± 0.06	10.72 ± 0.22	10 ± 5	57.0 ± 1.4	12	3.30 ± 0.27	17.3 ± 1.3

depth of about 1.60 m below the modern surface (Figure 2a) close to sample CH02/2/5, dated to 13.7±1.0 ka. The lower OSL sensitivity of this sample (Figure 2c) places it at the end of the period of high sedimentation. Sediment accumulation rates of 0.10 m/ka and 0.60 m/ka were calculated for the Holocene and Pleistocene sediments, respectively. The value for the Holocene can be compared with the value of 0.2 m/ka at Duowa (DW in Figure 1), calculated for the period of 12 to 2.5 ka (Roberts *et al*., 2001); this was the value for deposition prior to the period of increased dust production related to agricultural expansion in adjacent areas. By carrying out a regression of age on depth down the section at Yuanbao, and observing a sudden change in the regression coefficient, the change in sedimentation rate was located at a depth of 1.61 m and an age of 13.48±1.15 ka was calculated for this depth. This change in rate of dust deposition (Figure 2a) is far better defined than either the start of the colour change (at about 2.4 m, 15.1±1.7 ka, which is the average of ages of samples CH02/2/7 and CH02/2/8) or the boundary based on the mid-point of the MS measurements (at about 1.3 m, 9.8±0.7 ka of sample CH02/2/4) as a boundary for the P/H transition in this section (Figure 2b).

Discussion

The change in OSL sensitivity and the change in sedimentation rate determined from the OSL ages occurred simultaneously at a depth of close to 1.6 m at this section at Yuanbao. The cause of the change in OSL sensitivity could be related to a change in source material, brought about by a change in the wind direction of the winter monsoon. This change could be related to rapid movement of the desert/loess boundary (Zhou *et al*., 2002) and a related change in the source material. The change in sedimentation rate should be interpreted in terms of a change in wind strength, or to a change in availability of source material. The timing for this change in sedimentation rate was calculated to be 13.48±1.15 ka, placing it a little later than the first increase in ice accumulation rate in Greenland at 14 680± 400 yr BP (GISP2 timescale), at the end of the cold period known as the Older Dryas (Alley *et al*., 1993). In a previous study at Yuanbao, Chen *et al*. (1997) showed that between 1 and 2 m depth there was a factor of two change in the percentage of grains with a diameter greater than 40 μm. Unfortunately, no grain size data were available for this OSL-dated section at Yuanbao. Changes in wind strength have been proposed as the cause of changes in grain size during the last 130 ka at several sites in the centre of the CLP (Zhang *et al*., 1994).

The new values for the sedimentation rates can be used to calculate mass accumulation rates (MARs) that are used to test the output of global climate models (Kohfeld and Harrison, 2003). A recent survey of the literature for the CLP (Sun *et al*., 2000) has been used to estimate MARs for Marine Isotope Stages (MIS) 5 to 1 (Kohfeld and Harrison, 2003). At Yuanbao, Kohfeld and Harrison (2003) calculated MARs of 208 and 1055 g/m^2 per yr for MIS 1 (the Holocene) and MIS 2 (the end of the Pleistocene), respectively, based on the data summarised by Sun *et al*. (2000), taken from Chen *et al*. (1996, 1997, 1999). Based on the new OSL ages, the MARs at Yuanbao can be re-calculated from the sedimentation rates. Using the value of sediment bulk density of 1.48 g/cm^3 (Kohfeld and Harrison, 2001, 2003), the MIS1 MAR at Yuanbao is 148 g/m^2 per yr, and the MIS2 MAR is 888 g/m^2 per yr. The new values are slightly smaller than those given by Kohfeld and Harrison (2003).

The increase in MS was seen to start at a depth of about 2.4 m, at a point where there was a visible colour change in the field (Figure 2b). One explanation for this could be postdepositional alteration of the loess underlying the Holocene soil, as suggested for the last interglacial soil (S_1) at several sites in this part of China (Wu *et al*., 2002; Feng *et al*., 2004b; Liu *et al*., 2004). However, it is possible that climatic warming may have started earlier than the beginning of the Holocene, being recorded as a slight increase in the MS values and a weak colour change. At Dadongling section (DDL in Figure 1), Chen *et al*. (1995) measured MS at 1 cm intervals and found two peaks below the main Holocene increase, with the lowest having an estimated age of 14.3 ka; this would support the hypothesis of a pre-Holocene warming (F. Oldfield, personal communication, 2006). At Yuanbao, the age of the onset of the MS increase is 15.5±1.3 ka at a depth of 2.4 m. It is thus possible that syn-depositional pedogenesis occurs as the climate warms, even though the high sedimentation rate (0.60 m/ka) continues for a further 1000–2000 years.

Conclusions

From OSL measurements of quartz grains from a section at Yuanbao, it has been possible to establish the position of the Pleistocene/Holocene boundary in this section and its timing in this part of China. This has been achieved by using the OSL ages to calculate the sedimentation rates for the Holocene and the end of the Pleistocene. In addition, an increase in OSL sensitivity was found for the sediment above this boundary. This change in OSL sensitivity is proposed to be related to a change in dust source.

The P/H boundary, defined by the change in sedimentation rate, was found at a depth of 1.61 m, about 30 cm lower in the section than the MS-defined boundary and about 80 cm above the boundary defined by colour change in the field. This can be explained either in terms of pedogenic penetration into the L_1 loess or by a gradually warming climate occurring before the sedimentation rate changed. This ambiguity suggests that, although low-field MS measurement can be used for providing a chronology for the loess deposits on a Quaternary timescale, care should be taken if using it for high-resolution palaeoclimate reconstruction, or for construction of indirect chronologies.

An age of 13.48±1.15 ka was obtained for the change in sedimentation rate at the P/H boundary. The sedimentation rates derived from the OSL ages were used to recalculate the mass accumulation rates for MIS 1 and MIS 2 at this site and provide confirmation for those previously deduced. The new values imply that there is a factor of six decrease in dust deposition from the glacial to interglacial for the latest MIS stages (1 and 2).

Acknowledgements

Thanks are due to Professor Cao Jixiu and Dr Chen Yimeng for help in the field, Professor Chen Fahu for bringing this site to our attention and logistical help for field work, Dr Richard Bailey for the spreadsheet for D_e calculation, Professor Geoff Duller for the spreadsheet for age calculation, Ms Ailsa Allen for help to draw Figure 1, and Dr Francis Marriot for help in error calculation related to determining the age of the break in sedimentation rate. We wish to thank the referees for helpful comments on the manuscript. ZPL thanks Oxford University for a Clarendon Scholarship of full support of his DPhil study, and Jesus College, Oxford University, for grants for fieldwork.

References

Alley, R.B., Meese, D.A., Shuman, C.A., Gow, A.J., Taylor, K.C., Grootes, P.M., White, J.W.C., Ram, M., Waddington, E.D., Mayewski, P.A. and **Zielinski, G.A.** 1993: Abrupt increase in snow accumulation at the end of the Younger Dryas event. *Nature* 362, 527–29.

An, Z.S. 2000: The history and variability of the East Asian paleomonsoon climate. *Quaternary Science Reviews* 19, 171–87.

An, Z.S. and **Porter, S.C.** 1997: Millennial-scale climatic oscillations during the last interglaciation in central China. *Geology* 25, 603–606.

An, Z.S., Kukla, G.J., Porter, S.C. and **Xiao, J.L.** 1991: Magnetic susceptibility evidence of monsoon variation on the Loess Plateau of central China during the last 130 000 years. *Quaternary Research* 36, 29–36.

Bailey, R.M., Bray, H. and **Stokes, S.** 2003: Inductively-Coupled Plasma Mass Spectrometry (ICP-MS) for dose rate determination: some guidelines for sample preparation and analysis. *Ancient TL* 21, 11–14.

Berger, G.W., Mulhern, P.J. and **Huntley, D.J.** 1980: Isolation of silt-sized quartz from sediments. *Ancient TL* 11, 8–9.

Bøtter-Jensen, L., Bulur, E., Duller, G.A.T. and **Murray, A.S.** 2000: Advances in luminescence instrumentation. *Radiation Measurements* 32, 523–28.

Chen, F.H., Wu, R.J., Pompei, D. and **Oldfield, F.** 1995: Magnetic property and particle size variations in the late Pleistocene and Holocene parts of the Dadongling loess section near Xining, China. *Quaternary Proceedings* 4, 27–40.

Chen, F.H., Ma, Y.Z. and **Li, J.J.** 1996: High resolution record of Malan Loess in the Longxi Loess Plateau and rapid climate changes during the last glaciation (in Chinese). *Journal of Glaciology and Geocryology* 18, 111–18.

Chen, F.H., Bloemendal, J., Wang, J.M., Li, J.J. and **Oldfield, F.** 1997: High-resolution multi-proxy climate records from Chinese loess: evidence for rapid climatic changes over the last 75 kyr. *Palaeogeography, Palaeoclimatology, Palaeoecology* 130, 323–35.

Chen, F.H., Bloemendal, J., Feng, Z.D., Wang, J.M., Parker, E. and **Guo, Z.T.** 1999: East Asian monsoon variations during Oxygen Isotope Stage 5: evidence from the northwestern margin of the Chinese loess plateau. *Quaternary Science Reviews* 18, 1127–35.

Chen, J., Ji, J.F., Balsam, W., Chen, Y., Liu, L.W. and **An, Z.S.** 2002: Characterization of the Chinese loess-paleosol stratigraphy by whiteness measurement. *Palaeogeography, Palaeoclimatology, Palaeoecology* 183, 287–97.

Ding, Z., Yu, Z., Rutter, N.W. and **Liu, T.** 1994: Towards an orbital time scale for Chinese loess deposits. *Quaternary Science Reviews* 13, 39–70.

Derbyshire, E., Keen, D.H., Kemp, R.A., Rolph, T.A., Shaw, J. and **Meng, X.M.** 1995: Loess-palaeosol sequences as recorders of palaeoclimatic variations during the last glacial interglacial cycle: some problems of correlation in north-central China. *Quaternary Proceedings* 4, 7–18.

Fang, X.M., Ono, Y., Fukusawa, H., Pan, B.T., Li, J.J., Guan, D.H., Oi, K., Tsukamoto, S., Torii, M. and **Mishima, T.** 1999: Asian summer monsoon instability during the past 60 000 years: magnetic susceptibility and pedogenic evidence from the western Chinese Loess Plateau. *Earth and Planetary Science Letters* 168, 219–32.

Feng, Z.-D., Wang, H.-B. and **Olson, C.G.** 2004a: Pedogenic factors affecting magnetic susceptibility of the last interglacial palaeosol S_1 in the Chinese Loess Plateau. *Earth Surface Process and Landforms* 29, 1389–402.

Feng, Z.D., Wang, H.B., Olson, C., Pope, G.A., Chen, F.H., Zhang, J.W. and **An, C.B.** 2004b: Chronological discord between the last interglacial paleosol (S_1) and its parent material in the Chinese Loess Plateau. *Quaternary International* 117, 17–26.

Heller, F., Shen, C.D., Beer, J., Liu, X.M., Liu, T.S., Bronger, A., Suter, M. and **Bonani, G.** 1993: Quantitative estimates of pedogenic ferromagnetic mineral formation in Chinese loess and palaeoclimatic implications. *Earth and Planetary Science Letters* 114, 385–90.

Imbrie, J., Hays, J.D., Martinson, D.G., McIntyre, A., Mix, A.C., Morley, J.J., Pisias, N.G., Prell, W.L. and **Shackleton, N.J.** 1984: The orbital theory of Pleistocene climate: support from a revised chronology of the marine $\delta^{18}O$ record. In Berger, A.L., Hays, J.D, Kukla, G. and Salzman, B., editors, *Milankovitch and climate, part 1*. Reidel, 269–305.

Jain, M., Murray, A.S. and **Bøtter-Jensen, L.** 2003: Characterisation of blue-light stimulated luminescence components in different quartz samples: implications for dose measurement. *Radiation Measurements* 37, 441–49.

Kemp, R.A. 2001: Pedogenic modification of loess: significance for palaeoclimatic reconstructions. *Earth Science Reviews* 54, 145–56.

Kohfeld, K.E. and **Harrison, S.P.** 2001: DIRTMAP: the geological record of dust. *Earth Science Reviews* 54, 81–114.

—— 2003: Glacial–interglacial changes in dust deposition on the Chinese Loess Plateau. *Quaternary Science Reviews* 22, 1859–78.

Kukla, G. 1987: Loess stratigraphy in central China. *Quaternary Science Reviews* 6, 191–219.

Kukla, G. and **An, Z.** 1989: Loess stratigraphy in Central China. *Palaeogeography, Palaeoclimatology, Palaeoecology* 72, 203–25.

Kukla, G., Heller, F., Liu, X.M. and **Xu, T.C.** 1988: Pleistocene climates in China dated by magnetic susceptibility. *Geology* 16, 811–14.

Liu, Q.S., Banerjee, S.K., Jackson, M.J., Chen, F.H., Pan, Y.X. and **Zhu, R.X.** 2004: Determining the climatic boundary between the Chinese loess and palaeosol: evidence from aeolian coarse-grained magnetite. *Geophysical Journal International* 156, 267–74.

Liu, T.S. 1985: *Loess and the environment*. China Ocean Press, 251 pp.

Lu, H.Y., Liu, X.D., Zhang, F.Q., An, Z.S. and **Dodson, J.** 1999: Astronomical calibration of loess–paleosol deposits at Luochuan, central Chinese Loess Plateau. *Palaeogeography, Palaeoclimatology, Palaeoecology* 154, 237–46.

Maher, B.A. and **Taylor, R.H.** 1988: Formation of ultrafine-grained magnetite in soils. *Nature* 336, 368–70.

Maher, B.A., Thompson, R. and **Zhou, L.P.** 1994: Spatial and temporal reconstructions of changes in the Asian palaeomonsoon: a new mineral magnetic approach. *Earth and Planetary Science Letters* 125, 461–71.

Martinson, D.G., Pisias, N.G., Hays, J.D., Imbrie, J., Moore, T.C. and **Shackleton, N.J.** 1987: Age dating and orbital theory of the Ice Ages: development of a high-resolution 0 to 300 000 year chronostratigraphy. *Quaternary Research* 27, 1–29.

Murray, A.S. and **Wintle, A.G.** 2000: Luminescence dating of quartz using an improved single-aliquot regenerative-dose protocol. *Radiation Measurements* 32, 57–73.

—— 2003: The single aliquot regenerative dose protocol: potential for improvements in reliability. *Radiation Measurements* 37, 377–81.

Porter, S.C. 2000: High-resolution paleoclimatic information from Chinese eolian sediments based on grayscale intensity profiles. *Quaternary Research* 53, 70–77.

Porter, S.C. and **An, Z.S.** 1995: Correlation between climate events in the North Atlantic and China during the last glaciation. *Nature* 375, 305–308.

Prescott, J.R. and **Hutton, J.T.** 1994: Cosmic ray contributions to dose rates for luminescence and ESR dating: large depths and long-term time variations. *Radiation Measurements* 23, 497–500.

Pye, K. 1995: The nature, origin and accumulation of loess. *Quaternary Science Reviews* 14, 653–67.

Rees-Jones, J. 1995: Optical dating of young sediments using fine-grain quartz. *Ancient TL* 13, 9–13.

Roberts, H.M. and **Wintle, A.G.** 2001: Equivalent dose determination for polymineral fine-grains using the SAR protocol: application to a Holocene sequence of the Chinese Loess Plateau. *Quaternary Science Reviews* 20, 859–63.

Roberts, H.M., Wintle, A.G., Maher, B.A. and **Hu, M.Y.** 2001: Holocene sediment-accumulation rates in the western Loess Plateau, China, and a 2500-year record of agricultural activity, revealed by OSL dating. *The Holocene* 11, 477–83.

Sun, J.M., **Kohfeld, K.E.** and **Harrison, S.P.** 2000: *Records of aeolian dust deposition on the Chinese Loess Plateau during the Late Quaternary.* Technical Reports, Max-Planck-Institut fur Biogeochemie, 318 pp.

Watanuki, T., **Murray, A.S.** and **Tsukamoto, S.** 2003: A comparison of OSL ages derived from silt-sized quartz and polymineral grains from Chinese loess. *Quaternary Science Reviews* 22, 991–97.

Wu, G.J., **Pan, B.T.**, **Guan, Q.Y.**, **Liu, Z.G.** and **Li, J.J.** 2002: Loess record of climatic changes during MIS5 in the Hexi Corridor, northwest China. *Quaternary International* 97–98, 167–72.

Xiao, J.L., **Porter, S.C.**, **An, Z.S.**, **Kumai, H.** and **Yoshikawa, S.** 1995: Grain size of quartz as an indicator of winter monsoon strength on the Loess Plateau of central China during the last 130 000 yr. *Quaternary Research* 43, 22–29.

Zhang, X.Y., **An, Z.S.**, **Chen, T.**, **Zhang, G.Y.**, **Arimoto, R.** and **Ray, B.J.** 1994: Late Quaternary records of the atmospheric input of eolian dust to the center of the Chinese Loess Plateau. *Quaternary Research* 41, 35–43.

Zhou, L.P., **Oldfield, F.**, **Wintle, A.G.**, **Robinson, S.G.** and **Wang, J.T.** 1990: Partly pedogenic origin of magnetic variations in Chinese loess. *Nature* 346, 737–39.

Zhou, W.J., **Dodson, J.**, **Head, M.J.**, **Li, B.S.**, **Hou, Y.J.**, **Lu, X.F.**, **Donahue, D.J.** and **Jull, A.J.T.** 2002: Environmental variability within the Chinese desert-loess transition zone over the last 20 000 years. *The Holocene* 12, 107–12.